Inorg. Chem. **2007**, *46*, 5787–5790

Low-Valent Vanadium Oxide Nanostructures with Controlled Crystal Structures and Morphologies

Guicun Li,* Kun Chao, Hongrui Peng, Kezheng Chen, and Zhikun Zhang

Key Laboratory of Nanostructured Materials, Qingdao University of Science and Technology, Qingdao 266042, People's Republic of China

Received February 21, 2007

Low-valent vanadium oxide nanostructures have been synthesized in large quantities using commercial V_2O_5 powder as the precursor by a facile reduction method. The crystal structures and morphologies of vanadium oxide nanostructures can be adjusted by altering the concentrations and types of reductants. VO_2(B) nanostructures are fabricated using oxalic acid as the reductant. VO_2(B) nanobelts with widths of 80–150 nm, thicknesses of 20–30 nm, and lengths up to several micrometers can evolve to olive-like nanostructures composed of nanosheets with thicknesses of several nanometers and lateral dimensions of several micrometers as the concentration of oxalic acid increases. $H_2V_3O_8$ nanobelts with widths of 200–300 nm, thicknesses of 10–20 nm, and lengths up to several 10s of micrometers are obtained under the reduction of V_2O_5 powder with ethanol. The belt-shaped morphologies of $H_2V_3O_8$ are not affected by the concentration of ethanol.

Introduction

Low-dimensional nanostructures including those of zero dimension, one dimension, and two dimension have exhibited specific physical and chemical properties due to their dimensions of nanometer-size magnitude, which differs greatly from that of their bulk counterparts.[1,2] Vanadium oxides are of interest due to their redox activity and layered structures, which can be inserted by various intercalation species.[3,4] Among them, some low-valent vanadium oxides are very unique. For example, VO_2 can undergo a first-order transition from a high-temperature metallic phase to a low-temperature insulating phase at around 340 K[5,6] and exhibits excellent optical, electrical, and electrochemical properties.[5,7−10] In recent years, there has been increasing interest in low-dimensional vanadium oxide nanostructures because of their size-dependent properties[11−13] and potential applications in lithium batteries,[14−16] electric field-effect transistors,[17,18] chemical sensors or actuators,[19−21] and nanodevices.[22] Considerable efforts have been devoted toward the fabrication

* To whom correspondence should be addressed. E-mail: guicunli@qust.edu.cn. Tel: 86-532-84022869. Fax: 86-532-84022869.

(1) Alivisatos, A. P. *Science* **1996**, *271*, 933−934.
(2) Murray, C. B.; Norris, D. J.; Bawendi, M. G. *J. Am. Chem. Soc.* **1993**, *115*, 8706−8715.
(3) Murugan, A. V.; Kwon, C. W.; Campet, G.; Kale, B. B.; Mandale, A. B.; Sainker, S. R.; Gopinath, C. S.; Vijayamonhanan, K. *J. Phys. Chem. B* **2004**, *108*, 10736−10742.
(4) Pang, S.; Li, G.; Zhang, Z. *Macromol. Rapid Commun.* **2005**, *26*, 1262−1265.
(5) Morin, F. J. *Phys. Rev. Lett.* **1959**, *3*, 34−36.
(6) Biermann, S.; Poteryaev, A.; Lichtenstein, A. I.; Georges, A. *Phys. Rev. Lett.* **2005**, *94*, 026404.
(7) Manning, T. D.; Parkin, I. P.; Pemble, M. E.; Sheel, D.; Vernardou, D. *Chem. Mater.* **2004**, *16*, 744−749.
(8) Goodenough, J. B. *J. Solid State Chem.* **1971**, *3*, 490−500.
(9) Li, W.; Dahn, J. R.; Wainwright, D. S. *Science* **1994**, *264*, 1115−1118.
(10) Murphy, D. W.; Christian, P. A.; Carides, J. N. *J. Electrochem. Soc.* **1979**, *126*, 497−499.
(11) Lopez, R.; Feldman, L. C.; Haglund, R. F. *Phys. Rev. Lett.* **2004**, *93*, 177403.
(12) Lopez, R.; Haynes, T. E.; Boatner, L. A.; Feldman, L. C.; Haglund, R. F. *Phys. Rev. B: Condens. Matter Mater. Phys.* **2002**, *65*, 224113.
(13) Lopez, R.; Haglund, R. F.; Feldman, L. C.; Boatner, L. A.; Haynes, T. E. *Appl. Phys. Lett.* **2004**, *85*, 5191−5193.
(14) Dobley, A.; Ngala, K.; Yang, S.; Zavalij, P. Y.; Whittingham, M. S. *Chem. Mater.* **2001**, *13*, 4382−4386.
(15) Li, G.; Pang, S.; Jiang, L.; Guo, Z.; Zhang, Z. *J. Phys. Chem. B* **2006**, *110*, 9383−9386.
(16) Qiao, H.; Zhu, X.; Zheng, Z.; Liu, L.; Zhang, L. *Electrochem. Commun.* **2006**, *8*, 21−26.
(17) Kim, G. T.; Muster, J.; Krstic, V.; Park, J. G.; Park, Y. W.; Roth, S.; Burghard, M. *Appl. Phys. Lett.* **2000**, *76*, 1875−1877.
(18) Muster, J.; Kim, G. T.; Krstić, V.; Park, J. G.; Park, Y. W.; Roth, S.; Burghark, M. *Adv. Mater. (Weinheim, Ger.)* **2000**, *12*, 420−424.
(19) Liu, J.; Wang, X.; Peng, Q.; Li, Y. *Adv. Mater. (Weinheim, Ger.)* **2005**, *17*, 764−767.
(20) Gu, G.; Schmid, M.; Chiu, P. W.; Minett, A.; Fraysse, J.; Kim, G. T.; Roth, S.; Kozlov, M.; Muñoz, E.; Baughman, R. H. *Nat. Mater.* **2003**, *2*, 316−319.
(21) Biette, L.; Carn, F.; Maugey, M.; Achard, M. F.; Maquet, J.; Steunou, N.; Livage, J.; Serier, H.; Backov, R. *Adv. Mater. (Weinheim, Ger.)* **2005**, *17*, 2970−2974.
(22) Myung, S.; Lee, M.; Kim, G. T.; Ha, J. S.; Hong, S. *Adv. Mater. (Weinheim, Ger.)* **2005**, *17*, 2361−2364.

10.1021/ic070339n CCC: $37.00 © 2007 American Chemical Society
Published on Web 06/05/2007

of low-valent vanadium oxide nanostructures by a variety of methods, such as thermal evaporation, surfactant-assisted solution, and hydrothermal/solvothermal synthesis. Park et al.[23,24] synthesized monoclinic VO_2 nanowires with a rectangular cross section using a vapor transport method. Baudrin et al.[25] prepared a three-dimensional network of monoclinic VO_2 filaments by heating vanadium oxide aerogels under vacuum. Li et al.[26] reported the fabrication of monoclinic VO_2 single-crystalline nanobelts by a hydrothermal reaction between formic acid and ammonium metavanadate. Qian et al.[27] reported an ethylene glycol reduction process to prepare monoclinic VO_2 nanowire arrays under hydrothermal conditions. Nesper et al.[28] developed a two-step method to synthesize mixed-valent vanadium oxide (VO_x) nanotubes using aliphatic amines as surfactants: a gel formed by hydrolysis and nanotubes generated by hydrothermal treatment. Our group has synthesized orthorhombic $H_2V_3O_8$ single-crystalline nanobelts by a hydrothermal method in the presence of hydrochloric acid.[29] In the solution-based synthesis, the formation of low-valent vanadium oxides is usually dependent on reductants and only one-dimensional nanostructures are formed. However, the synthesis of two-dimensional nanostructures remains challenging to chemists and material researchers. Some organic molecules, such as oxalic acid and ethanol, show different reduction abilities in organic chemistry, which inspired us to adjust the valences of vanadium oxides. Herein, we report a facile reduction approach to the synthesis of low-valent vanadium oxide nanostructures with controlled crystal structures and morphologies by altering the concentrations and types of reductants.

Experimental Section

Synthesis of Low-Valent Vanadium Oxide Nanostructures. 0.36 g of commercial V_2O_5 powder was added to 80 mL oxalic acid (or ethanol) in aqueous solution with different concentrations to form a yellow slurry. The slurry was stirred for 10 min and then transferred to a 100 mL autoclave with a Teflon liner. The autoclave was maintained at 180 °C for 24 h and then air-cooled to room temperature. The resulting dark blue precipitates were collected and washed with distilled water and ethanol several times and then dried at 60 °C under vacuum for 10 h. In all reactions, the content of the commercial V_2O_5 powder is kept unchanged.

Characterization. The morphologies and sizes of the resulting products were characterized by field-emission scanning electron microscopy (FE-SEM, JSM 6700F) and transmission electron microscopy (TEM, JEM 2000EX). The crystal structures of the resulting products were characterized by powder X-ray diffraction (XRD, Rigaku D-max-γA XRD with Cu Kα radiation, $\lambda = 1.54178$ Å).

(23) Guiton, B. S.; Gu, Q.; Prieto, A. L.; Gudiksen, M. S.; Park, H. *J. Am. Chem. Soc.* **2005**, *127*, 498−499.
(24) Wu, J.; Gu, Q.; Guiton, B. S.; Leon, N. P.; Ouyang, L.; Park, H. *Nano Lett.* **2006**, *6*, 2313−2317.
(25) Baudrin, E.; Sudant, G.; Larcher, D.; Dunn, B.; Tarascon, J. M. *Chem. Mater.* **2006**, *18*, 4369−4374.
(26) Liu, J.; Li, Q.; Wang, T.; Yu, D.; Li, Y. *Angew. Chem., Int. Ed.* **2004**, *43*, 5048−5052.
(27) Chen, X.; Wang, X.; Wang, Z.; Wan, J.; Liu, J.; Qian, Y. *Nanotechnology* **2004**, *15*, 1685−1687.
(28) Spahr, M. E.; Bitterli, P.; Nesper, R.; Müller, M.; Krumeich, F.; Nissen, H. U. *Angew. Chem., Int. Ed.* **1998**, *37*, 1263−1265.
(29) Li, G.; Pang, S.; Wang, Z.; Peng, H.; Zhang, Z. *Eur. J. Inorg. Chem.* **2005**, 2060−2063.

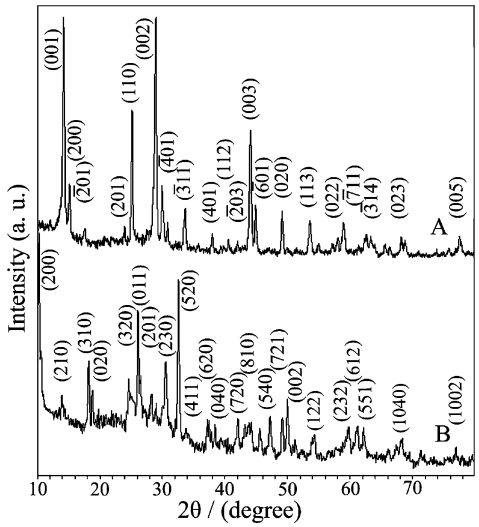

Figure 1. XRD patterns of low-valent vanadium oxide nanostructures synthesized with different reductants at 180 °C for 24 h. (A) oxalic acid, VO_2(B); (B) ethanol, $H_2V_3O_8$.

Results and Discussion

Figure 1 shows the XRD patterns of powder made of low-valent vanadium oxide nanostructures synthesized with different reductants at 180 °C for 24 h. As shown in Figure 1A, the diffraction peaks of the resulting products synthesized using oxalic acid as reductant can be indexed to monoclinic crystalline phase VO_2(B) with lattice contents $a = 12.1$ Å, $b = 3.70$ Å, $c = 6.43$ Å, and $\beta = 107.0°$ (JCPDS 812392, Table S1, see the Supporting Information), revealing that the V^{5+} ions in V_2O_5 have been reduced to V^{4+} ions by oxalic acid in the reaction. In addition, when ethanol is used as the reductant, the diffraction peaks of the products can be ascribed to orthorhombic crystalline phase $H_2V_3O_8$ with lattice contents $a = 16.9$ Å, $b = 9.36$ Å, and $c = 3.64$ Å (JCPDS 852401, Table S2, see the Supporting Information), indicating that the V^{5+} ions in V_2O_5 are reduced partly to V^{4+} ions by ethanol.

The influences of the concentrations and types of reductants on the morphologies of low-valent vanadium oxide nanostructures have been investigated. Figure 2 presents typical SEM and TEM images of VO_2 nanobelts synthesized with 0.05 mol/L oxalic acid at 180 °C for 24 h. As shown in the low-magnification SEM image (Figure S1, see the Supporting Information), one can observe that the products are composed of a large quantity of one-dimensional VO_2 nanostructures with typical lengths of up to several micrometers. In a high-magnification SEM image in Figure 2A, it is clear that the geometrical shape of the VO_2 nanostructures is a belt. The thicknesses and widths of VO_2 nanobelts are about 20−30 nm and 80−150 nm, respectively. Some VO_2 nanobelts have irregular edges. The TEM image in Figure 2B confirms the belt-shaped morphology of VO_2. The sizes of the nanobelts are consistent with that in Figure 2A. The electron diffraction (ED) taken from an individual nanobelt (the inset in Figure 2B) indicates that the nanobelt is a single crystal and can grow along the [010] direction.

The concentration of oxalic acid plays an important role in controlling the morphologies of VO_2 nanostructures. As

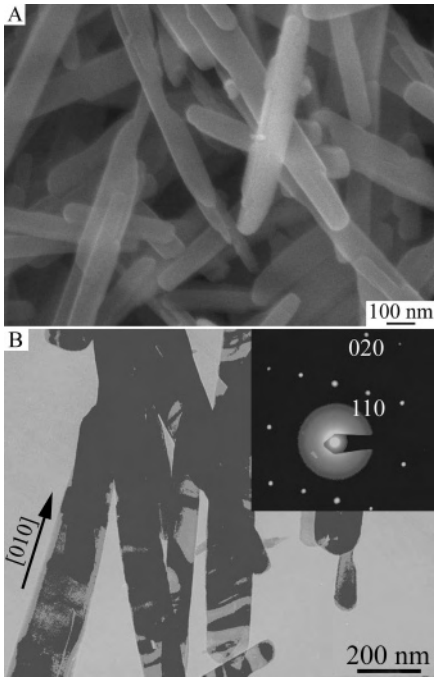

Figure 2. SEM and TEM images of VO_2 nanobelts synthesized with 0.05 mol/L oxalic acid at 180 °C for 24 h. (A) high-magnification SEM image; (B) TEM image. The inset in Figure 2B shows a typical ED pattern taken from an individual nanobelt.

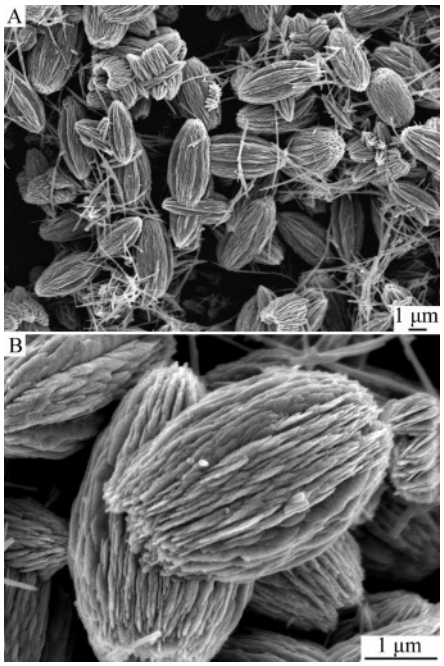

Figure 3. SEM images of VO_2 nanostructures synthesized with 0.08 mol/L oxalic acid at 180 °C for 24 h. (A) low-magnification SEM image; (B) high-magnification SEM image.

the concentration of oxalic acid increases to 0.08 mol/L, as shown in Figure 3A and its low-magnification SEM image (Figure S2, see the Supporting Information), it is interesting to note that the products are made up of a large amount of olive-like VO_2 nanostructures and a small amount of nanowires. The lengths and aspect ratios of the olives are about several micrometers and 2:1, respectively. The high-magnification SEM image in Figure 3B reveals that the olive-like nanostructures consist of many VO_2 nanosheets with

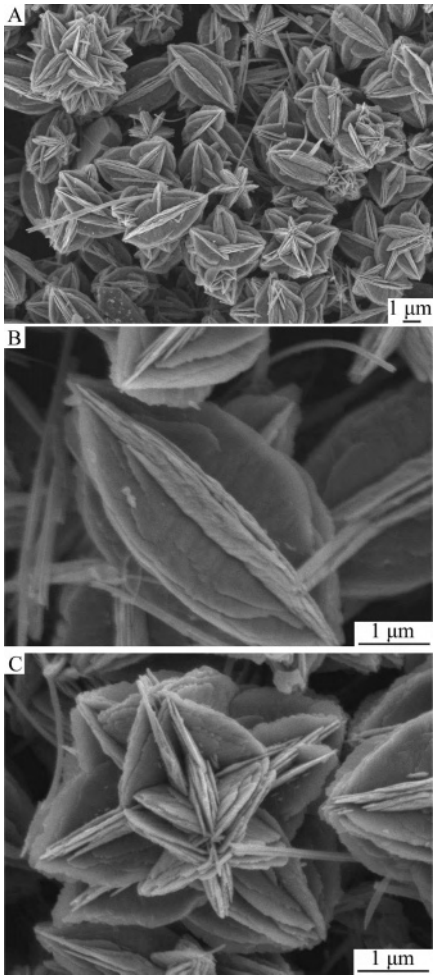

Figure 4. SEM images of VO_2 nanostructures synthesized with 0.10 mol/L oxalic acid at 180 °C for 24 h. (A) low-magnification SEM image; (B and C) high-magnification SEM images.

thicknesses of 10−20 nm and lateral dimensions of several micrometers. The nanosheets are very closely aligned along the axis of the olive-like structure. Figure 4 shows typical SEM images of VO_2 nanostructures synthesized with 0.10 mol/L oxalic acid at 180 °C for 24 h. It is found that olive-like nanostructures with six petals (Figure 4A) are formed. The sizes are similar to that in Figure 3. In a high-magnification SEM image (Figure 4B), it can be seen that each petal is composed of several nanosheets. Compared with Figure 3, the thickness of nanosheets decreases to several nanometers and their lateral dimensions are several micrometers. Interestingly, as shown in Figure 4C, some hierarchical structures with sixfold symmetry composed of nanosheets can also be formed in the products.

When ethanol is used as the reductant, orthorhombic crystalline phase $H_2V_3O_8$ is obtained (Figure 1B). Figure 5 represents typical SEM and TEM images of $H_2V_3O_8$ nanobelts synthesized with 1.0 mol/L ethanol at 180 °C for 24 h. As shown in Figure 5A, a large amount of $H_2V_3O_8$ nanobelts are formed in the green precipitates. The typical widths and lengths of the nanobelts are in the range of 200−300 nm and several 10s of micrometers, respectively. The high-magnification SEM image in Figure 5B reveals that the products are belt-shaped and the thicknesses are about 10−

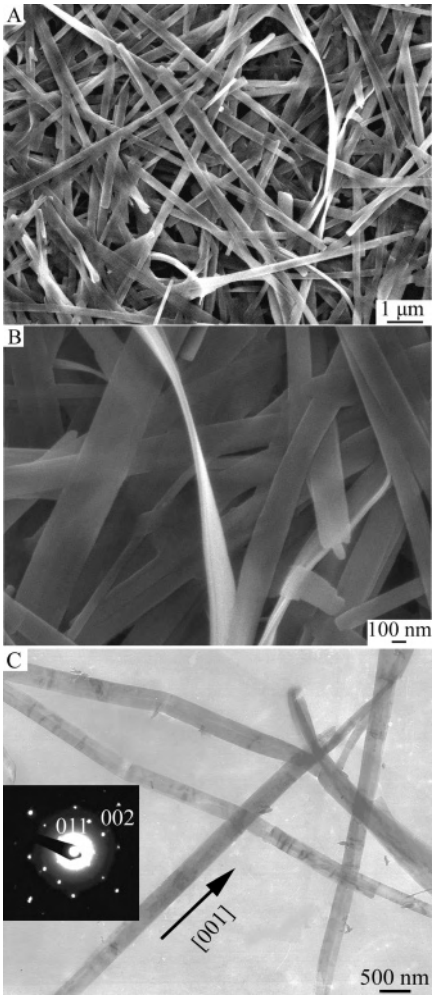

Figure 5. SEM and TEM images of $H_2V_3O_8$ nanobelts synthesized with 1.0 mol/L ethanol at 180 °C for 24 h. (A) low-magnification SEM image; (B) high-magnification SEM image; (C) TEM image. The inset in Figure 5C shows a typical ED pattern recorded from a single nanobelt.

20 nm. The TEM image in Figure 5C confirms that the products have belt-shaped structures. The ED pattern recorded from a single nanobelt (the inset in Figure 5C) indicates that the nanobelts are single crystalline and the growth occurs along the [001] direction. The belt-shaped morphologies of $H_2V_3O_8$ are not affected by the concentrations of ethanol. As shown in Figure 6, $H_2V_3O_8$ nanobelts are synthesized easily with 0.5 and 1.5 mol/L ethanol at 180 °C for 24 h. In comparison with Figure 5, the widths, thicknesses, and lengths of $H_2V_3O_8$ nanobelts change little as the concentration of ethanol increases.

The solution-based synthesis of low-valent vanadium oxide nanostructures is free of any surfactants. The basic reactions for low-valent vanadium oxide nanostructures can be expressed as

$$V_2O_5 + C_2H_2O_4 = 2VO_2 + 2CO_2 + H_2O$$

$$3V_2O_5 + CH_3CH_2OH + H_2O = 2H_2V_3O_8 + CH_3CHO$$

It is supposed that the formation of belt- and sheet-shaped nanostructures is related to the layered structures of vanadium oxides. In the beginning of the reaction, V_2O_5 can be dissolved partly in the reductant aqueous solution. Under

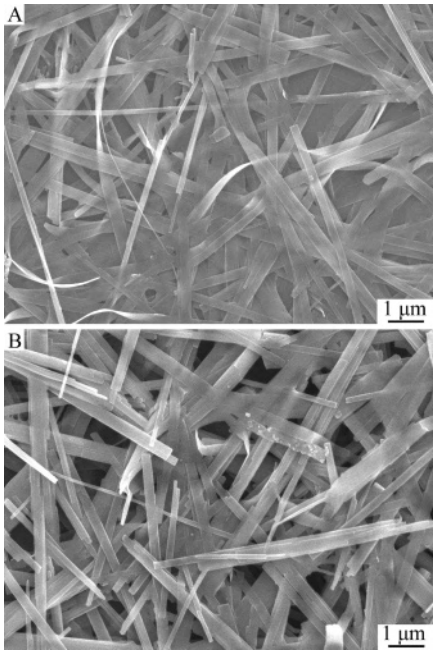

Figure 6. SEM images of $H_2V_3O_8$ nanobelts synthesized with different concentrations of ethanol at 180 °C for 24 h. (A) 0.5 mol/L; (B) 1.5 mol/L.

hydrothermal conditions, the reductants, such as oxalic acid and ethanol, have different reduction abilities, so the V^{5+} ions in V_2O_5 are reduced partly or completely to V^{4+} to form VO_2 and $H_2V_3O_8$ nanocrystals, which can serve as the growth sites for the formation of VO_2 and $H_2V_3O_8$ nanostructures. The difference between oxalic acid and ethanol is that oxalic acid can act as a bidendate ligand able to modify the surfaces of growing nanocrystals, particularly the surface that possesses the lower electronic density, thus avoiding specific surface growth and providing the observed morphology difference when adjusting the oxalate counterion concentration. As ethanol does not possess the above bidendate capabilities, the final nanocrytals morphology will be not affected by the concentration of ethanol.

Conclusion

In summary, we have demonstrated a facile reduction route to the large-scale synthesis of low-valent VO_2(B) and $H_2V_3O_8$ nanostructures using commercial V_2O_5 powder as the precursor. VO_2(B) nanobelts are fabricated by the reduction of oxalic acid, which can evolve to olive-like nanostructures composed of nanosheets as the concentration of oxalic acid increases from 0.05 to 0.10 mol/L. $H_2V_3O_8$ nanobelts are synthesized by the reduction of ethanol, and the belt-shaped morphologies of $H_2V_3O_8$ are not affected by the concentration of ethanol.

Acknowledgment. This work was supported by the Research Fund for the Doctoral Program of Qingdao University of Science and Technology, People's Republic of China.

Supporting Information Available: Low magnification SEM image of VO_2 nanostructures and the indexed powder patterns for VO_2(B) and $H_2V_3O_8$. This material is available free of charge via the Internet at http://pubs.acs.org.

IC070339N